A Novel Circularly Polarized Fan-Beam Antenna for 5.8 GHz DSRC Applications

Stefano Maddio[*]

Abstract—This paper presents a novel compact printed antenna exploitable for Dedicated Short-Range Communication at 5.8 GHz. The design of the proposed device is based on the concentric arrangement of two contemporary fed patches operating with different modes. The resulting antenna exhibits a fan-beam pattern, with a wide lobe in one plane and narrow lobe in the plane perpendicular to the former, while retaining exceptionally small dimensions. The actual width of the beam makes the antenna suitable to cover a single road lane, as prescribed by the Intelligent Transportation System framework requirements. Furthermore, it natively operates in Circular Polarization, as prescribed by the ETSI EN 302 663 normative. Experimental validations demonstrate that the proposed antenna presents a Left-Hand gain of 4.1 dB at center frequency, with HPBW_x and HPBW_y equal to 160° and 45°, respectively, showing good agreement with the simulations. This measured performance confirms that the device is adequate to cover a single road-lane, according to the European framework for Dedicated Short-Range Communication for traffic monitoring.

1. INTRODUCTION

In the last years the need for sustainable mobility has been the driving force of the Intelligent Transportation Systems (ITS) framework [1]. The latter is capable of dealing with traffic efficiency and management, drive safety, accident management, etc. Antennas are obviously key components of ITS, being the enabling technology for Radio-Frequency Identification. In this context, radio links in Circular Polarization (CP) are preferred, given their inherent capability to contrast the multipath impairment [2, 3], as well as their ability to communicate regardless of the reciprocal angle between transmitter and receiver.

A fixed node of the ITS communication system, usually labeled as Road Side Unit (RSU), typically needs to monitor a single road lane. As a consequence, its antenna has to radiate a specific gain pattern, with a wide lobe in one plane and a narrow lobe in the plane perpendicular to the former. Its radiation diagram can be called a *Fan-Beam* shape.

A particularly interesting case scenario is that of free-flow applications, where there is no physical barrier to stop the car while collecting information from the On-Board Unit (OBU). In this case, the engagement area has to be the longest possible in the travel direction to grant the best communication performance despite the fast movement of the vehicle. To facilitate this it is desirable to have a wide fan-beam pattern characterized by very different requirements for the half power angle in the two directions, to grant the coverage of a single road line. This shape is generally obtained with complex array architectures, which usually need equally complicated feeding networks and are characterized by a large area occupation.

The possibility of reconfiguring the operational area, passing from a large to a narrower footprint, is also a feature of interest for RSU. This fact implies that the antenna is capable of radiating both a

fan beam and a directive beam, which in turn imposes additional constraints on the type of antenna and the corresponding feeding network, which can be very challenging [4].

On top of this, the design is even more challenging if the need of circular polarization is considered.

In view of these considerations, this paper proposes an innovative design for a CP antenna operating at 5.8 GHz, suitable for the coverage of a single lane. The antenna pattern realizes the required beam shape exploiting the modal combination of two very simple patches, designed to operate in two different modes, but at the same frequency. Both of them operate in modal degeneration, radiating a circularly polarized signal using a single feed. When the two patches are excited by two signals with the same amplitude and phase, the modal recombination results in a gain pattern with a wide fan-beam shape. Hence, the feeding network of the antenna is very simple, becoming a single Wilkinson power divider.

Furthermore, with the simple addition of a different kind of power splitter instead of the single Wilkinson power divider — such as the one used in [5] — the proposed antenna is also the perfect candidate for the future development of reconfigurable front-ends.

Experimental validations of a realized prototype in an anechoic setup demonstrate that the proposed antenna presents a Left-Hand (LH) gain of 4.1 dB at center frequency. The half-power angles in the principal cuts, labeled as $HPBW_x$ and $HPBW_y$, are 160° and 45°, respectively. These values are suitable for a free-flow single-lane implementation. In addition, the device presents a polarization ratio exceeding 15 in the bore-sight direction and a return loss in excess of −15 dB, making it adequate to operate according to the European framework of Dedicated Short-Range Communication (DSRC) for traffic monitoring.

2. ANTENNA DESIGN

The proposed antenna is based on the concentric arrangement of two disc-based patches. This architecture is similar to the one presented by the author in [6]. In the cited paper, the two patches are used to create multiple beams for Space Division Multiple Access (SDMA) applications, while here the different characteristics of the two modes are exploited for the synthesis of a specific shape pattern.

The two patches are based on the mechanism of modal degeneration for CP generation, but operate in two different resonant modes. The key to obtain the modal degeneration is to exploit a quasi-symmetric shape. The process used to obtain the two elements of the array is presented in the following subsections.

2.1. Patch #1

The first patch is based on the design proposed by the author in [7] and is hereby briefly described.

With reference to Figure 1(a), this patch consists of a disc which is centrally cut by an elliptical shape with axes $A \times B$. There is no closed form expression for this kind of design. However, it is quite easy to synthesize this patch choosing the disc radius R_1 to have a device resonating in the fundamental TM_{11} at the central frequency of 5.8 GHz. Subsequently, the disc geometry is perturbed with a central elliptical cut, with axes A and B, in order to cause the modal degeneration.

(a)   (b)   (c)
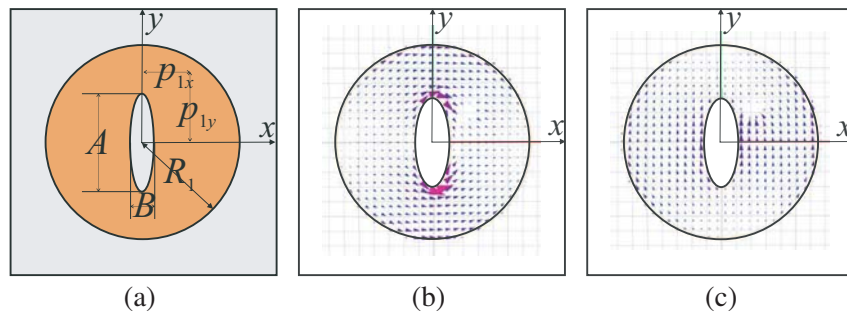
Figure 1. Pictorial representation of the first patch and its resonant modes. (a) Antenna layout. (b) Even mode. (c) Odd mode.

According to the well-known approximate relation valid for the regular disc patch, the disc radius R_1 and resonant frequency f_0 must satisfy [8]:

$$\begin{cases} f_0 = f_{mn} = \dfrac{\chi_{mn} c}{2\pi \widetilde{R_1} \sqrt{\varepsilon_r}} \\[4mm] \widetilde{R_1} = R_1 \sqrt{1 + \dfrac{2t}{\pi R_1 \varepsilon_r} \left(\ln \dfrac{\pi R_1}{2t} + 1.7726 \right)} \end{cases} , \qquad (1)$$

where χ_{mn} are the roots of the equation $J'(x) = 0$, i.e., the zeros of the derivative of the n-th Bessel function of the first kind, and t is the substrate thickness (1.575 mm). For the fundamental mode, the results are $mn = 11$ and $\chi_{11} = 1.841$.

Thus, the A and B elliptical cut is considered to serve as a degeneration driver. Hence the TM_{11} mode splits in two orthogonal and partially overlapped ones, labeled as TM_{1e} and TM_{1o}, resonating at f_{1e} and f_{1o}, respectively. Once the radius R_1 is fixed, the actual values of the two resonant frequencies are controlled by the ellipse dimensions A and B. A numerical characterization of the relationship linking the modal frequencies to the disc geometry is provided in [8].

The behavior of the corresponding modal functions, arbitrarily labeled as *even* and *odd*, are depicted in Figure 1(b) and Figure 1(c), respectively. Both of them resemble that of the unperturbed fundamental mode, hence similar Linearly Polarized (LP) far-fields are radiated. The nominal CP condition is attained when the parameter set composed of R_1, A, and B as well as the pin position (p_{x1}, p_{y1}) is adjusted to excite both the modes in phase quadrature and identical magnitude at an intermediate frequency between f_{1e} and f_{1o}.

The resulting antenna design, source of a directive CP beam, has been already implemented on mobile nodes for DSRC application [10, 11]. The typical performances for both co-polar and cross-polar components are reported in Figure 2.
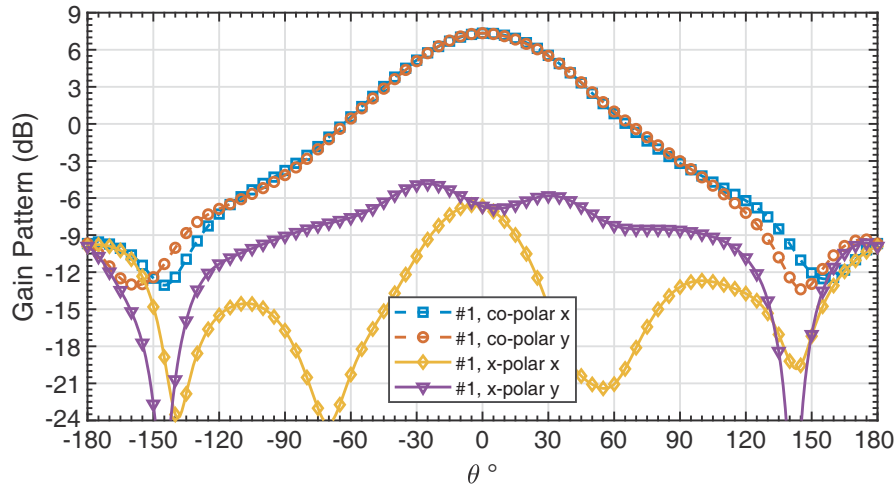

Figure 2. Gain pattern of Patch #1.

2.2. Patch #2

The second patch here considered operates according to the TM_{31} mode. This resonant mode is the source of a conic beam pattern with a deep broadside null (i.e., for $\theta = 0°$ and $\theta = 180°$) [8, 12].

To design a patch antenna operating in this mode, it is sufficient to choose a radius R_2 based on the value of χ_{31} in Eq. (1), i.e., 4.201. For this type of antenna, the magnetic-current distribution around the edge, proportional to the parameter n of the modes, undergoes three sinusoidal periods. As a consequence, to achieve CP operation, the geometry of this patch has to be modified exploiting a

multi-lobate curve compatible with the six-fold variation. Following the approach introduced in [6], the radius R_2 of the patch is modified here as the following curve:

$$\begin{cases} x(\theta, r) = R_2\left[(1 - r) + r\cos(6\theta)\right]\cos\theta \\ y(\theta, r) = R_2\left[(1 - r) + r\cos(6\theta)\right]\sin\theta \end{cases} \quad, \quad \theta \in [0, 2\pi], \tag{2}$$

where the r parameter dictates how this shape adds to or subtracts from the nominal value of R_2 around the circumference. Figure 3(a) shows this patch shape for various ripple amplitudes, expressed in percentage.
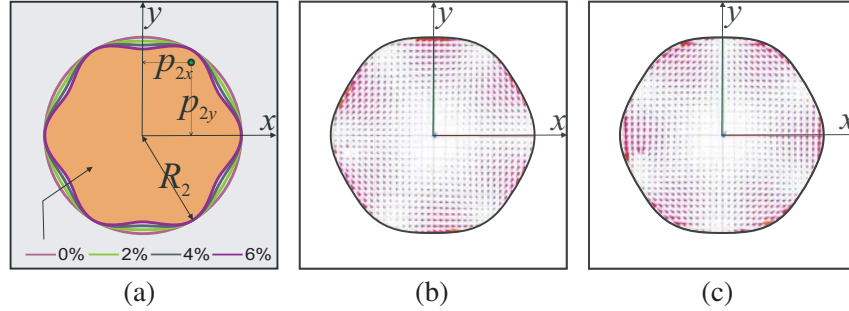

Figure 3. Pictorial representation of the second patch and its resonant modes. (a) Antenna layout. (b) Even mode. (c) Odd mode.

Exploiting this geometry the fundamental TM_{31} is therefore split into two degenerated modes, labeled TM_{3e} and TM_{3o}, depicted in Figure 3(b) and Figure 3(c), respectively. This ripple-based curve slightly perturbs the geometry of the modes while maintaining their overall field distribution by following the six-fold geometry of the unperturbed TM_{31} mode, similar to what the ellipse slit does for the inner patch and its fundamental TM_{11}.

Figure 4 shows how the previously described approach can also be applied to an annulus-shaped patch, obtained by practicing a central circular cut of the patch. The resultant antenna will still be a source of a conic beam with almost the same characteristics of the full patch, just with a lower gain due to the smaller active area. With reference to Figure 4(a), fixing the frequency of operation, the external radius R_2 and internal R_2' must satisfy a slightly more complex expression than the one presented in Eq. (1), but similar in nature.
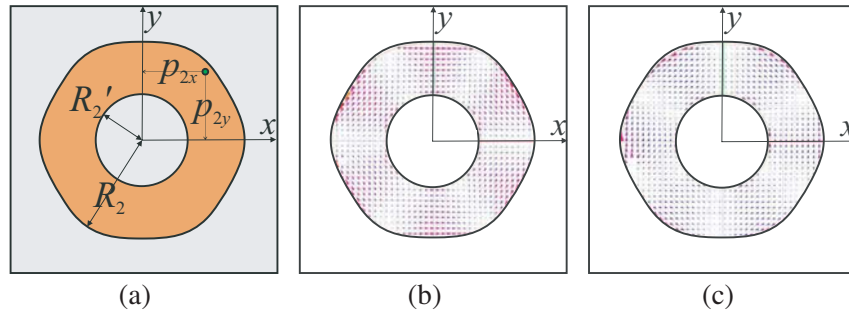

Figure 4. Pictorial representation of the annular shaped patch and its resonant modes. (a) Antenna layout. (b) Even mode. (c) Odd mode.

Once again, the multi-lobate curve is applied to the annulus external circumference to degenerate the resonant modes. With reference to Figure 4(b) and Figure 4(c), the modes responses in this configuration are very similar to the ones of the patch in Figure 3(b) and Figure 3(c), hence a similar radiative conic beam is expected.

As a side note, an advantage of the annular shape is the additional degree of freedom of R'_2, useful for tuning the resonant frequencies of the degenerated modes. However, the presence of the hole reduces the patch active area, hence limiting the efficiency and thus the maximum gain.

To better emphasize this fact, Figure 5 depicts the simulated patterns of #2 with and without the central hole. In either case, the design is adjusted to show the best performance at center frequency. Observing the figure it is evident that the conical shape of the pattern is the same in both cases, with similar co-polar and cross-polar components, confirming the complementary behavior with respect to the case of #1.
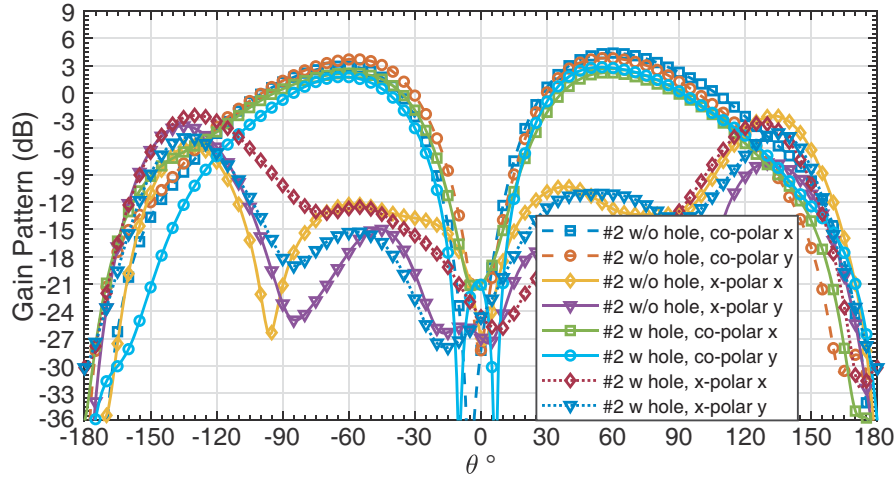

Figure 5. Gain pattern of Patch #2, with and without the central hole.

Indeed, the maximum gain is slightly different in the two cases: 3.5 dB for the case with the center hole and 2.3 dB in the case without it, as expected due to the presence of the central hole.

3. ANTENNA ASSEMBLY

Among the methods for the synthesis of a fan-beam there are those that use dielectric lens [13], those that exploit numerical synthesis [14], or those based on the opportune shape of the reflectors [15, 16].

Here, the fan-beam is obtained combining the directive beam pattern of #1 with the conical beam pattern of #2, and the approach is similar to the one proposed in [17]. To obtain a satisfactory fan-beam, an appropriate relative phase in the recombination of the fields is necessary.

Considering the complementary shape of the two patches, it is possible to arrange the first one inside the other, which is the reason for the annular design. The assembly is successful if the radius R_1 of the first patch is made smaller than the internal radius R'_2 of the second antenna. A gap between the two shapes is considered, making $R'_2 = R_1 + g$.

However, coupling between the patches is unavoidable due to the close proximity. Indeed, the gap g between the antennas must be narrow; otherwise, it would be impossible to synthesize the modal response of the outer patch, if the inner radius is too large.

Due to the strong proximity coupling, it is difficult to predict the exact modal recombination, even if the modal responses of each patch are obtained after a full-wave simulation. That said, even though the two antennas taken alone are designed to exhibit perfect polarization and a regular pattern, iterative re-tuning of the combined design is necessary when being combined.

In view of the final optimization, all the geometric parameters of the two patches are considered, including the pin positions (p_{1x}, p_{1y}) and (p_{2x}, p_{2y}).

A very important geometric parameter to consider when patches are arranged together is the orientation angle of the inner patch relative to the outer one, named α. This is illustrated in Figure 6(a), where the resulting layout for the proposed antenna is presented. This angle controls the relative phase
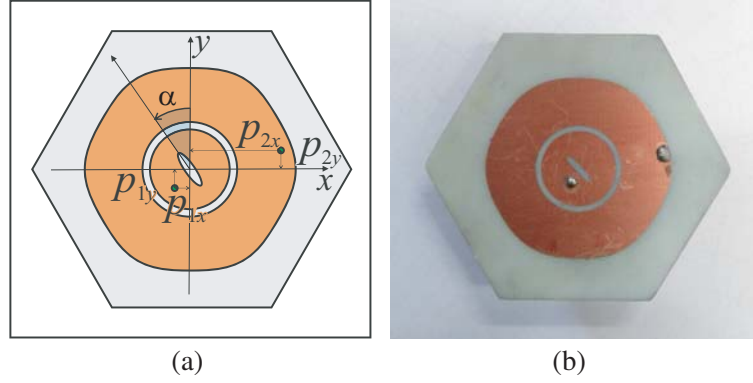
Figure 6. Layout and photograph of the proposed antenna prototype. (a) Layout. (b) Photograph.

of the patches, which is one of the most important parameters for proper field recombination. This parameter serves as the phase recombination parameter cited at the beginning of this section.

With this additional parameter, the final assembly of the patch is optimized, starting from the best solution found with a trial and error method. It is assumed that the patch is fed with a signal characterized by equal magnitude and phase, with this being one of the goals of this paper. A standard Wilkinson power divider is enough for the feeding of the device.

The geometrical dimensions after the optimization are presented in Table 1. It is worthwhile to report that the area of the antenna is $0.25\lambda_0^2$.

Table 1. List of the geometric parameters of the antenna design. All dimensions are in mm, all angles in degree.

R_1	A	B	p_{x1}	p_{y1}	α	R_2	R_2'	r	p_{x3}	p_{y3}
6.84	3.21	0.57	0.89	2.44	44.6°	16.87	7.77	1.25	14.99	3.24

The 3D polar plot of the properly fed array is shown in Figure 7(a). The actual combination after the final tuning is a fan-beam, as expected.

With reference to Figure 7(b) and following the approach presented in [18], the simulated pattern is projected to estimate the effects in an actual ETC application scenario, considering the antenna hanged
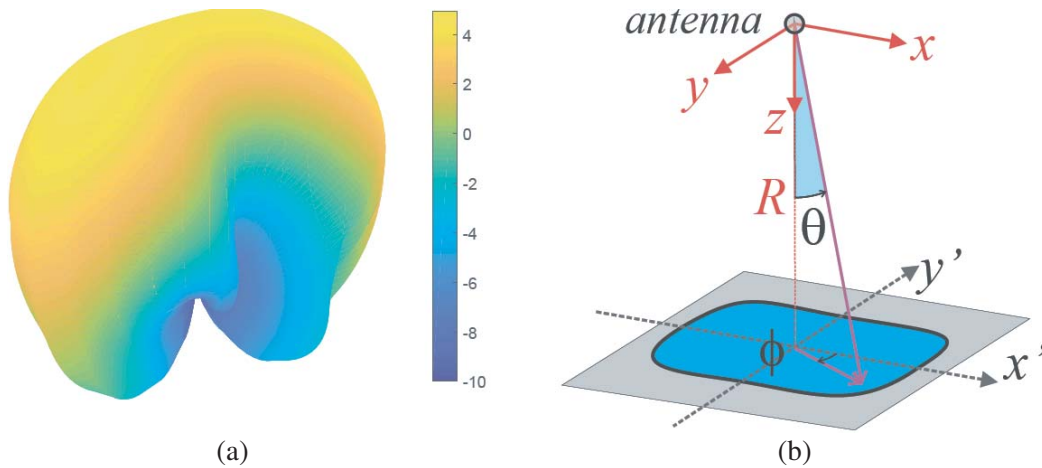

Figure 7. Antenna 3D pattern and setup for the projection. (a) Simulated 3D gain pattern. (b) Communication area.

from a gate placed at 5 m, pointing downward. A first-order propagation model is considered, without any bounce or scattering. This assumption is justified by the adoption of CP, which immunizes the link from the multipath.

In these conditions, the simulated footprint shown in Figure 8 demonstrates the effectiveness of the proposed approach. Considering an EIRP of 33 dBm, as prescribed by the norms [1], the maximum projected power is -29.2 dBm. The dotted line delimits the area where the ripple is less than 3 dB. This area can be approximated as a (3.5×10) m^2 rectangle. This optimal communication area very well follows the profile of a road line, which is highlighted by a pair of dashed lines.
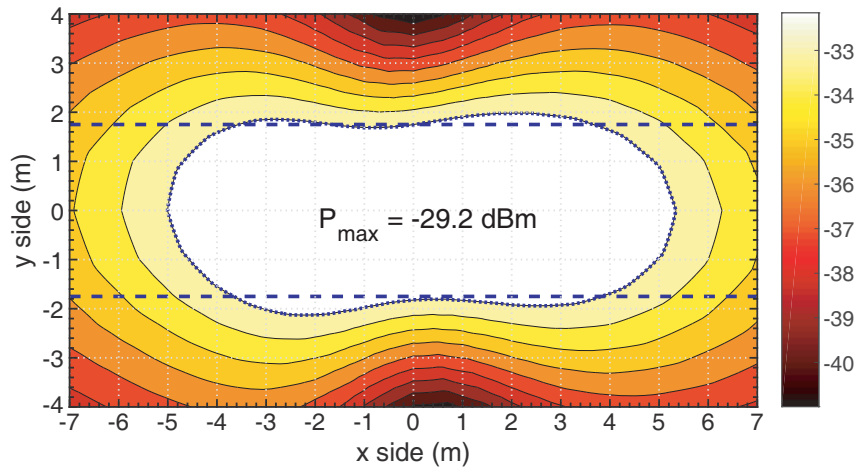

Figure 8. Footprint of the antenna pattern, depicted in Figure 7(a), projected according to the scheme in Figure 7(b).

Furthermore, the proposed device can also be used to produce the footprint illustrated in Figure 9 which is suitable for covering a road intersection.
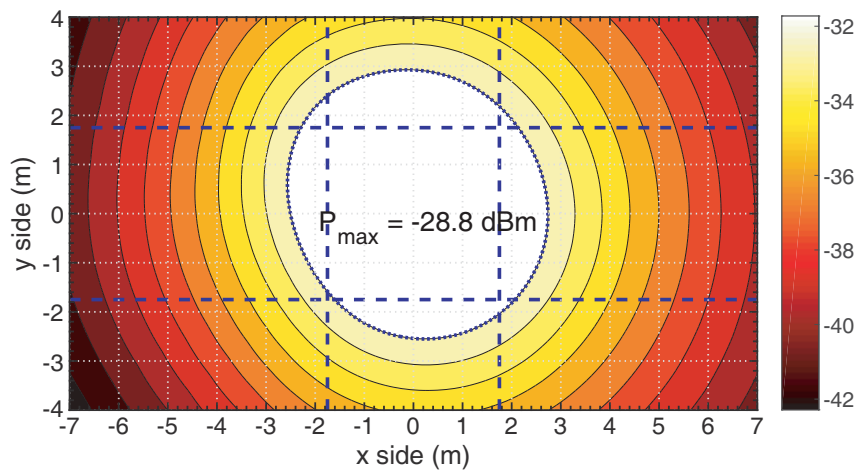

Figure 9. Footprint of the antenna pattern when only patch #1 is activated.

To achieve this effect it is sufficient to feed only patch #1, excluding patch #2. This can be done by means of a simple passive network consisting of a rat-race and a Wilkinson power divider, such as the one in [5].

The radiation efficiency of the antenna is estimated as 91% at central frequency, as can be seen in Figure 10. In addition, the efficiency is above 87% for a wide range of frequencies, confirming the effectiveness of the design, despite the issue of the #2 described in the previous section.
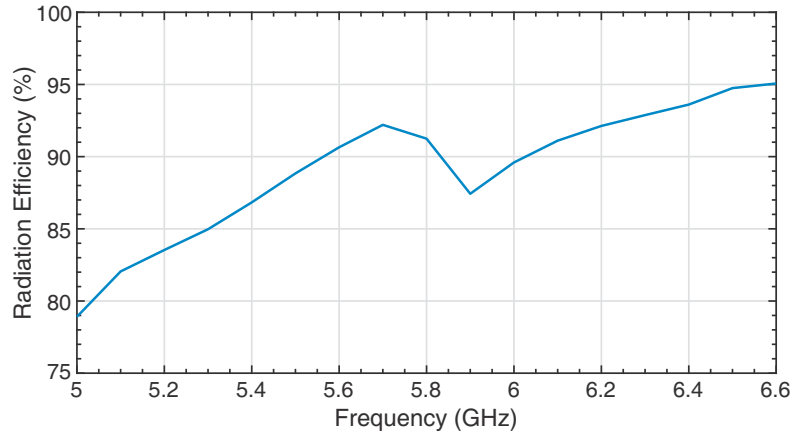
Figure 10. Efficiency of the proposed antenna.

4. EXPERIMENTAL VALIDATION

With reference to Figure 6(b), the design with the best performance has been fabricated, printed on a commercial dielectric substrate ($\varepsilon_r = 3.75$, $\tan\delta = 0.01$), and experimentally validated with the aid of a Vector Network Analyzer in an anechoic setup.

For the experimental characterization of the prototype, the Wilkinson power divider in Figure 11(a) was used. The assembling of the antenna, power divider, and cables are shown in Figure 11(b).
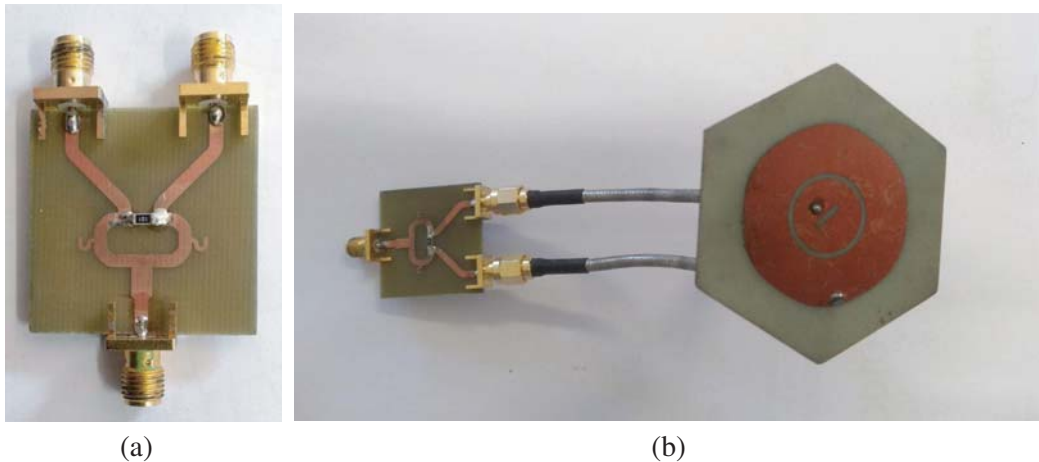

(a)   (b)

Figure 11. Photograph of the involved power divider and the assembled antenna prototype used for the experimental validation. (a) Wilkinson power divided (feeding network). (b) Assembled antenna prototype including the power divider and the cables.

Figure 12 depicts the measured reflection coefficient of the prototype. A return loss of 10 dB is observed at center frequency for both the patches, as well as a coupling level below -40 dB. The figure also shows the reflection coefficient of both antennas fed by the Wilkinson power divider depicted in Figure 11(a). It is observed that the measured return loss is greater than 18 dB at 5.8 GHz.

Figure 13 depicts the pattern at the center frequency of 5.8 GHz in both the x-cut and y-cut, corresponding to the wide and narrow cuts of the fan-beam, respectively. Very good agreement between simulation and measurement is observed, with both the cuts well matched.

The measurement is obtained using a Wilkinson Power Divider and a pair of equally long cables, and the gain value is amended by the feeding network loss to permit a fair comparison. There is
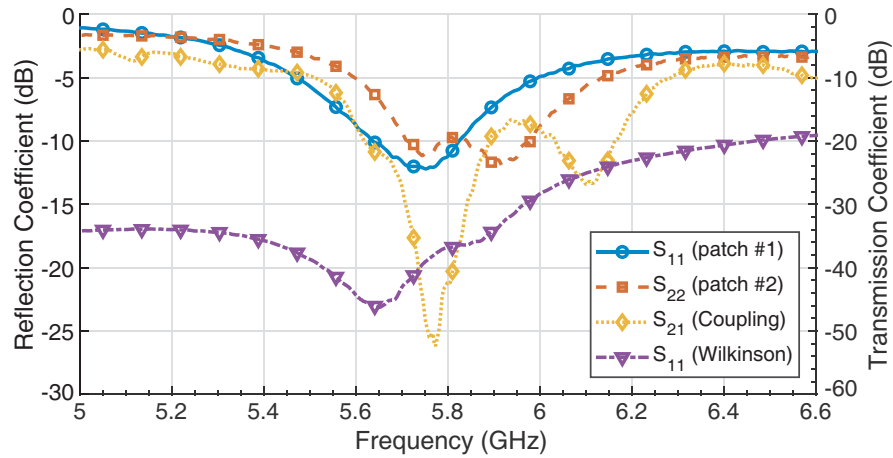
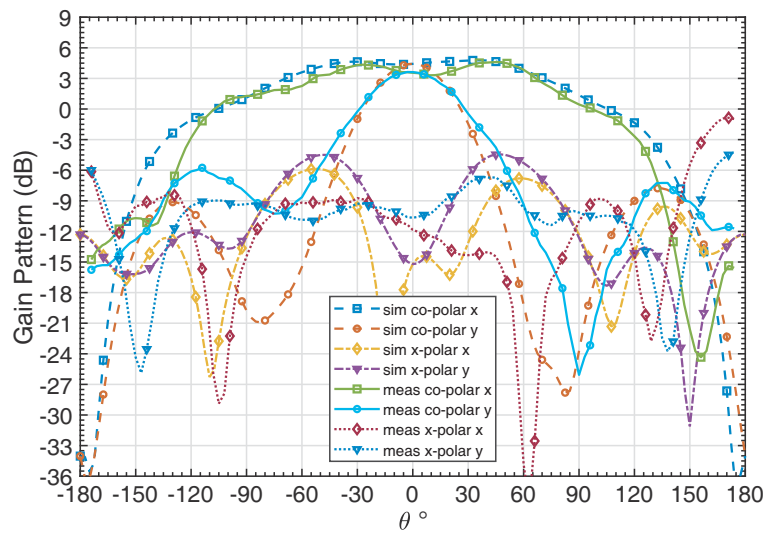**Figure 12.** Measured scattering parameter of the proposed antenna.

Figure 13. Simulated and measured gain pattern of the proposed antenna.
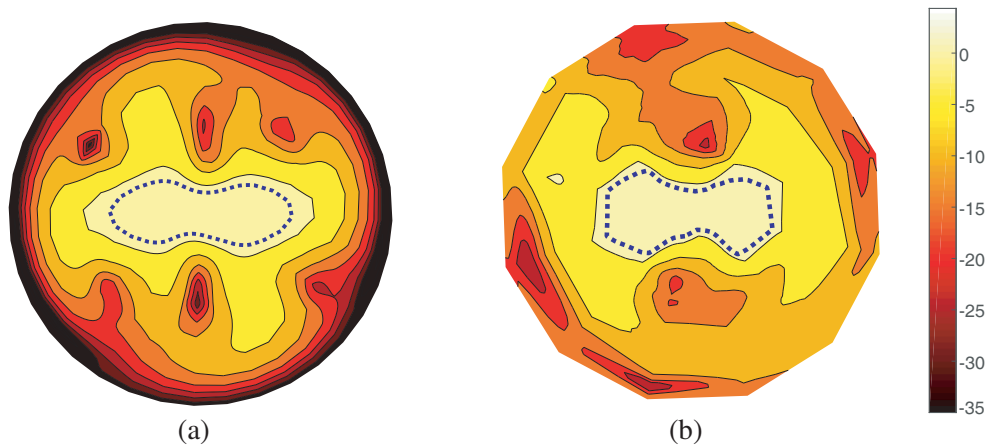

Figure 14. Simulated and measured 3D gain pattern of the proposed antenna. The dotted line identifies the region within 3 dB from the maximum. (a) Simulation. (b) Measurement.

a good agreement between simulation and measurement of the proposed antenna. In simulation, the boresight gain is 4.3 dB while the maximum gain is 4.6 dB. The measurements confirm 3.6 dB and 4.2 dB, respectively.

An $HPBW_x$ of 170° in simulation and 160° in measurement are observed. Almost identical values for 45°, meaning 45°, are observed in the two cases. The cross-polar component, while not identical, presents similar levels, below -10 dB in bore-sight direction.

Finally, Figure 14 shows the simulated and measured co-polar patterns, represented in 3D form. In the latter case, depicted in Figure 14(b), the pattern has been interpolated from 12 measured cuts. For both the data sets the angular region within 3 dB from the maximum is marked with a dotted line. Very good agreement is observed, especially comparing the peculiar shape of the main lobe.

5. CONCLUSION

A circularly polarized antenna radiating a fan-beam shape is proposed in this paper. Despite the compact dimension of $0.25\lambda_0^2$ at the central frequency of 5.8 GHz, the antenna behaves as an array, radiating a pattern with very different half power angles in the x and y axis directions.

Experimental validations demonstrate that the proposed device presents a maximum Left-Hand gain of 4.2 dB at center frequency, with $HPBW_x$ and $HPBW_y$ equal to 160° and 45°, respectively.

This feature and adequate circular polarization capability and the possibility to reconfigure the projected footprint make the device an adequate candidate in Dedicated Short-Range Communications, according to the European ETSI normative.

REFERENCES

1. ETSI, "302 663 v1. 2.1 intelligent transport systems (its); access layer specification for intelligent transport systems operating in the 5 GHz frequency band," *ETSI Standard*, 2013.
2. Chizhik, D., J. Ling, and R. A. Valenzuela, "The effect of electric field polarization on indoor propagation," *ICUPC'98, IEEE 1998 International Conference on Universal Personal Communications, Conference Proceedings (Cat. No. 98TH8384)*, Vol. 1, 459–462, IEEE, 1998.
3. Zhong, Z. and X. Liao, "Circular polarization benefits in outdoor to indoor scenarios for mimo cellular networks," *2014 Sixth International Conference on Wireless Communications and Signal Processing (WCSP)*, 1–5, IEEE, 2014.
4. Mohammadpour-Aghdam, K., R. Faraji-Dana, G. A. Vandenbosch, and W. De Raedt, "Fan and pencil beam aperture coupled patch antenna array with low side lobe level," *Proceedings of the Fourth European Conference on Antennas and Propagation*, 1–4, IEEE, 2010.
5. Maddio, S., A. Cidronali, M. Passafiume, G. Collodi, and S. Maurri, "Fine-grained azimuthal direction of arrival estimation using received signal strengths," *Electronics Letters*, Vol. 53, No. 10, 687–689, 2017.
6. Maddio, S., "A circularly polarized switched beam antenna with pattern diversity for WiFi applications," *IEEE Antennas and Wireless Propagation Letters*, Vol. 16, 125–128, 2016.
7. Maddio, S., A. Cidronali, I. Magrini, and G. Manes, "A design method for single-feed wideband microstrip patch antenna for switchable circular polarization," *2007 European Microwave Conference*, 262–265, IEEE, 2007.
8. James, J. R., P. S. Hall, et al., *Handbook of Microstrip Antennas*, Vol. 1, IET, 1989.
9. Maddio, S., "A compact wideband circularly polarized antenna array for C-band applications," *Antennas and Wireless Propagation Letters*, Vol. 14, 1081–1084, 2015.
10. Leonardi, O., M. G. Pavone, G. Sorbello, A. F. Morabito, and T. Isernia, "Compact single-layer circularly polarized antenna for short-range communication systems," *Microwave and Optical Technology Letters*, Vol. 56, No. 8, 1843–1846, 2014.
11. Maddio, S., "A compact circularly polarized antenna for 5.8-GHz intelligent transportation system," *IEEE Antennas and Wireless Propagation Letters*, Vol. 16, 533–536, 2016.

12. Garg, R., P. Bhartia, I. J. Bahl, and A. Ittipiboon, *Microstrip Antenna Design Handbook*, Artech house, 2001.

13. Hua, C., N. Yang, X. Wu, and W. Wu, "Millimeter-wave fan-beam antenna based on step-index cylindrical homogeneous lens," *IEEE Antennas and Wireless Propagation Letters*, Vol. 11, 1512–1516, 2012.

14. Steyskal, H., "On antenna power pattern synthesis," *IEEE Transactions on Antennas and Propagation*, Vol. 18, No. 1, 123–124, 1970.

15. Yurduseven, O. and D. Smith, "Symmetric/asymmetric *H*-plane horn fed offset parabolic reflector antenna with switchable pencil/fan-beam radiation characteristics," *ISAPE2012*, 82–85, IEEE, 2012.

16. Naghshvarianjahromi, M., "Novel Ku band fan beam reflector back array antenna," *Progress In Electromagnetics Research*, Vol. 3, 95–103, 2008.

17. Konishi, Y., M. Ohtsuka, M. Matsunaga, and S. Urasaki, "Fan-beam forming for a linear antenna with exponential-tapered amplitude distribution," *Electronics and Communications in Japan (Part I: Communications)*, Vol. 79, No. 10, 69–78, 1996.

18. Inserra, D., W. Hu, and G. Wen, "Antenna array synthesis for RFID-based electronic toll collection," *IEEE Transactions on Antennas and Propagation*, Vol. 66, No. 9, 4596–4605, 2018.